



## TEST ON FLEXURAL PERFORMANCE OF CIRCULAR CONCRETE-FILLED DOUBLE STEEL TUBULAR MEMBERS

Junchang Ci<sup>1</sup>, Mizan Ahmed<sup>2</sup>, Ahmed Hamoda<sup>3</sup>, Shicai Chen<sup>4</sup>

<sup>1</sup>PhD Student, Department of Civil Engineering, Beijing University of Technology, Beijing, China  
E-mail: [cjc\\_bjut@163.com](mailto:cjc_bjut@163.com)

<sup>2</sup>Academic, College of Engineering and Science, Victoria University, Melbourne, Australia  
E-mail: [Mizan.Ahmed@live.vu.edu.au](mailto:Mizan.Ahmed@live.vu.edu.au)

<sup>3</sup>Assistant Professor, Department of Civil Engineering, Kafrelsheikh University, Kafrelsheikh, Egypt

E-mail: [Ahmed\\_Hamoda@eng.kfs.edu.eg](mailto:Ahmed_Hamoda@eng.kfs.edu.eg)

<sup>4</sup>Professor, Department of Civil Engineering, Beijing University of Technology, Beijing, China  
E-mail: [chenshicai101@gmail.com](mailto:chenshicai101@gmail.com)

### ABSTRACT

This paper reports an experimental program performed to study the flexural performance of concrete-filled double steel tubular (CFDST) members composed of the circular section. A total of seven specimens including one conventional concrete-filled steel tubular (CFST) member and a double-skin concrete-filled steel tubular (DCFST) member were tested under pure bending load. The test parameters include the influences of the thickness of the outer and inner steel tube, diameter ratio, and concrete strengths. Test results show that CFDST members failed in a ductile manner under flexural load. The performance of CFDST members is influenced by the geometry and material properties of the members. However, the thickness of the outer steel tube is found to remarkably influence the flexural performance of CFDST members.

**Keywords:** CFDST members; circular section; composite members; flexural performance.

### INTRODUCTION

A circular **concrete-filled double steel tubular (CFDST) column** as shown in Fig. 1 offers **improved strength and ductility compared to conventional CFST and DCFST columns. This type of composite column can be also used to retrofit the conventional CFST column by placing an outer steel tube and fill the annulus with concrete. Although a significant amount of study has been performed to understand the performance of CFDST columns under different loading conditions, investigation on their flexural performance has not been reported yet. However, CFDST members can be subjected to large applied moment particularly in the region of high seismicity, hence should understand their behavior under bending is crucial for effective design purposes.**

Zheng and Tao [1], Ahmed et al. [2], and Ci et al. [3] studied the performance of circular short CFDST columns loaded concentrically. The axial compressive strength and ductility of square CFDST columns with inner circular tube have been investigated by Qian et al. [4], Ahmed et al. [5], and Ci et al. [6] while Xiong et al. [7] tested some double rectangular CFDST columns loaded concentrically. Furthermore, the mechanical performance of CFDST columns that are loaded eccentrically was examined by Ahmed et al. [8-10], Pei et al. [11], and Qian et al. [12].

Hassanein et al. [13] and Ahmed et al. [14, 15] further contributed to this research topic by investigating their global buckling behavior using numerical models. This paper reports a test program on the flexural performance of CFDST beams to examine the influences of the concrete compressive strength, the thickness of the steel tubes, and the diameter ratio.

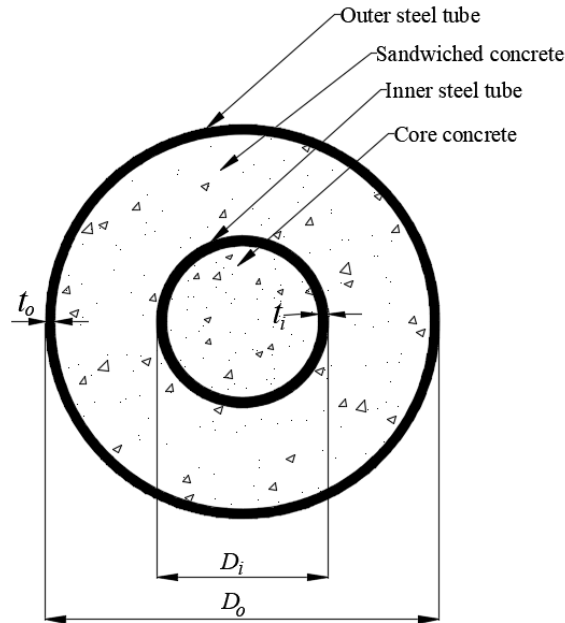


Fig. 1: A cross-sectional view of a circular CFDST specimen.

## TEST PROGRAM

### General

The test program comprised five CFDST members, one CFST, and one DCFST member subjected to flexural loading. The nominal diameter and length of all tested specimens were 219mm and 1400mm, respectively. Table 1 presents the details of the tested specimens. In naming the specimens in Table 1, the letter “CD” refers to CFDST members, “E” is the specimen used as the benchmark for comparison purposes, OT, IT, ID, and CS represent the changing parameters of the outer tube thickness, inner tube thickness, inner tube diameter, and concrete strength, respectively. Two different concrete strengths of C40 and C50 were used to fill the hollow sections of CFDST specimens.

### Material properties

The material properties of the steel tubes were measured from the tensile coupon test performed according to the Chinese standard GB/T 228-2010 [16]. Table 2 presents the measured average  $\pm$  standard deviation of the material properties of tensile coupon samples.

The compressive strength of concrete was measured using three (150mm $\times$ 150mm $\times$ 150mm) cube samples. The average cube strengths for C40 and C50 measured after 28 days were 47MPa and 60MPa, respectively.

Table 1: Summary of the geometry of the test specimens.

No.	Specimen label	Outer tube		Inner tube		L[mm]	$f'_{cu}$ [MPa]	$P_{Exp}$ [kN]
		$D_o$ [mm]	$t_o$ [mm]	$D_i$ [mm]	$t_i$ [mm]			
1	CFST	219	4	-	-	1400	47	622.67

2	DCFST	219	4	114	3.5	1400	47	658.34
3	CD-E	219	4	114	3.5	1400	47	650.56
4	CD-OT	219	5	114	3.5	1400	47	870.67
5	CD-IT	219	4	114	2.5	1400	47	676.67
6	CD-ID	219	4	140	3.5	1400	47	759.68
7	CD-CS	219	4	114	3.5	1400	60	772.96

**Table 2: Material properties of steel tubes.**

Tube type	No.	Geometry dimension $D \times t$ [mm]	$f_y$ (MPa)	$E_s$ (GPa)	$f_u$ (MPa)	$\varepsilon_u$
Outer tube	1	219×4	301.3±5.6	202.5±4.8	387.7±1.9	0.19±0.01
	2	219×5	331.7±6.9		416.9±2.6	0.15±0.01
Inner tube	3	114×2.5	314.4±5.2	199.1±3.8	375.3±2.5	0.19±0.01
	4	114×3.5	328.8±9.9		415.5±6.5	0.15±0.01
	5	140×3.5	331.4±7.3		396.4±5.5	0.13±0.01

### Test setup

The test program was conducted at the structural laboratory of Beijing University of technology. Figure 2 shows the schematic view of the test setup. The load is applied using a 400-ton universal testing machine to the upper end of specimens through the loading beam as shown in Fig. 3, thus forming the bending shear section with the bending moment and shear force at both ends of the test specimens, and the pure bending section (bending moment  $M = Pl_1/2$ ) in the middle of the span without shear force. Four semicircle hoops were used to ensure the stability of loading and preventing the lateral instability of specimens. Three linear variable differential transducers (LVDTs) were used to measure the vertical deflections at one-third of the span and the middle part of the span. The strain distributions were also measured using strain gauges.

The tested specimens were preloaded to 10kN prior to actual test loading to remove any possible gaps and to check the readings of strain gauges and LVDTs. The failure of the specimens was chosen when the maximum mid-span displacement reached 1/50 of the span, or when the load drops to 70% of the measured maximum load, or when the external steel tube had significant buckling deformation.

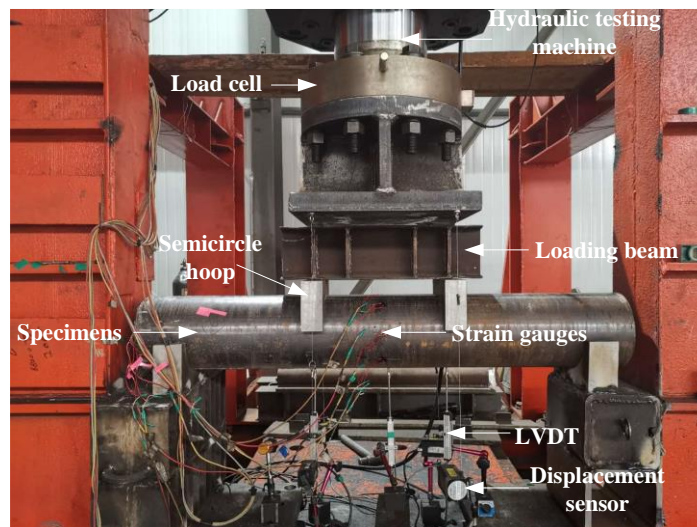


**Fig. 2: The overall view of the test device.**

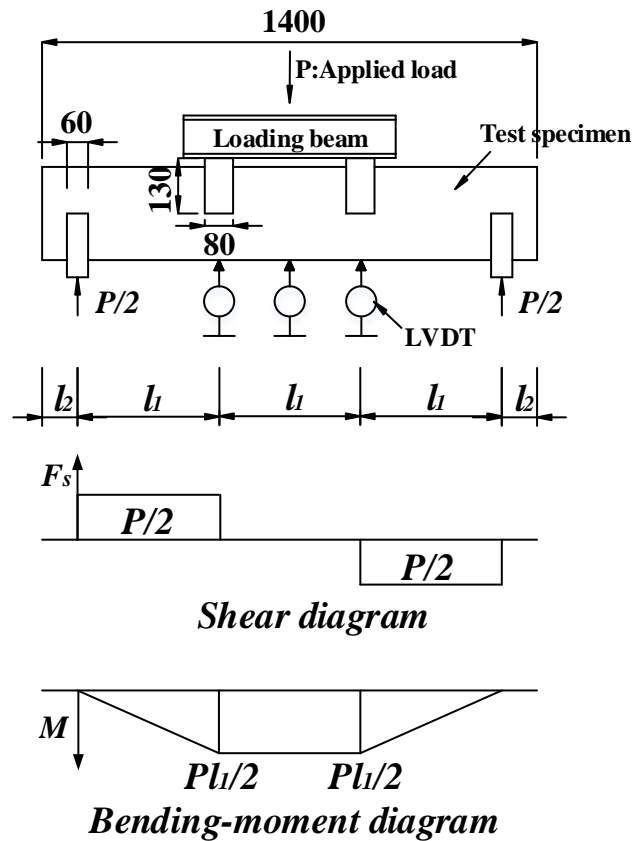


Fig. 3: Loading method.

## RESULTS AND DISCUSSIONS

Figures 4 and 5 show the failure patterns of the specimens where it can be seen that all specimens failed due to the flexural deformation. The local buckling of the steel tubes was observed at the compression zone between the two loading points. The failure of CFST and DCFST members was also similar to their CFDST counterparts as can be seen in Fig. 5. The bending moment ( $M$ ) and curvature ( $\phi$ ) of the members are calculated by Eq. (1) and Eq. (2), respectively, and plotted in Fig. 6.

$$M = PL/6 \quad (1)$$

$$\phi = \pi^2 u_m / L^2 \quad (2)$$

in which  $P$  is the load measured by the load cell;  $L$  is the effective length of the member, in this paper,  $L = 3l_1$ .  $u_m$  is the mid-span deflection of the member measured by LVDT.

The ultimate moment ( $M_{ue}$ ) of the member is taken as the maximum moment point whereas the yield points of specimens shown in redpoint were determined using the "farthest point method" proposed by Feng et al. [17].

From the  $M-\phi$  curves, it is seen that all the test members were in their elastic deformation stage at the early stage of loading and reached the plastic stage around 0.70-0.77 $M_{ue}$ .



Fig. 4: Failure modes of CFDST specimens.

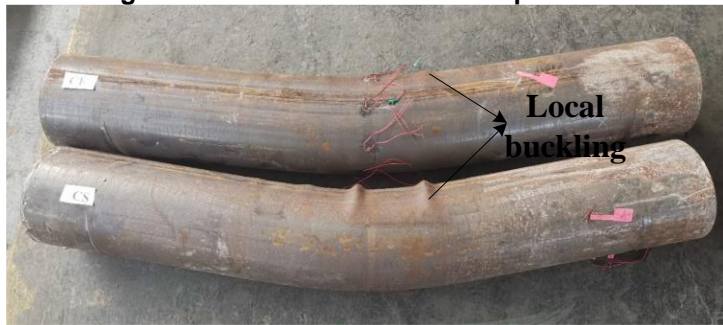
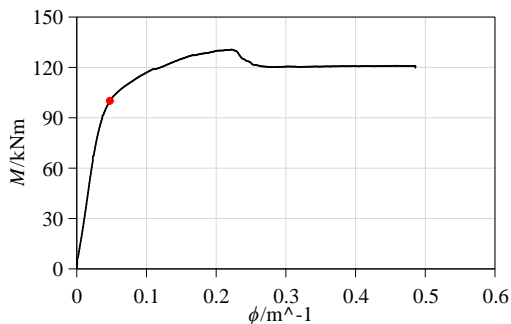
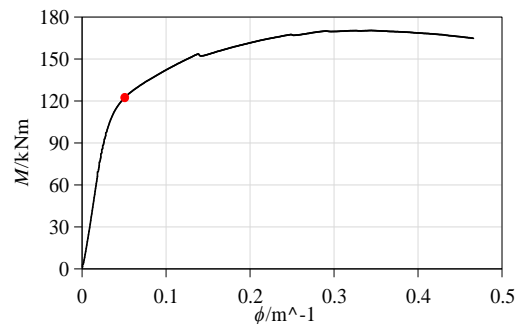


Fig. 5: Failure modes of CFST and DCFST specimens.

In analyzing the effects of various parameters, it is observed that increasing either the thickness of the steel tubes or the strength of concrete increases the ultimate moments of the specimens. However, the thickness of the external tube has the most remarkable influence on the flexural behavior of CFDST specimens compared to the other parameters. When the thickness of the outer tube increases from 4 to 5mm, the flexural capacity of the member increases by 33.8%. However, the increase in the flexural capacity is calculated as only about 4% when the thickness of the inner tube increases from 2.5mm to 3.5mm. When the concrete strength increases from 47 to 60 Mpa, the increase in the flexural capacity is calculated as 18.9%. In addition, the percentage of increase is estimated at 16.9% for the increase in the diameter of the inner tube from 114 to 140mm. Furthermore, the flexural performance of CFST, CFDST, and DCFST members is very similar. For example, the ultimate bending moment of CD-E is 4.48% higher than that of CFST and 1.20% lower than that of DCFST.



(a) CD-E



(b) CD-OT

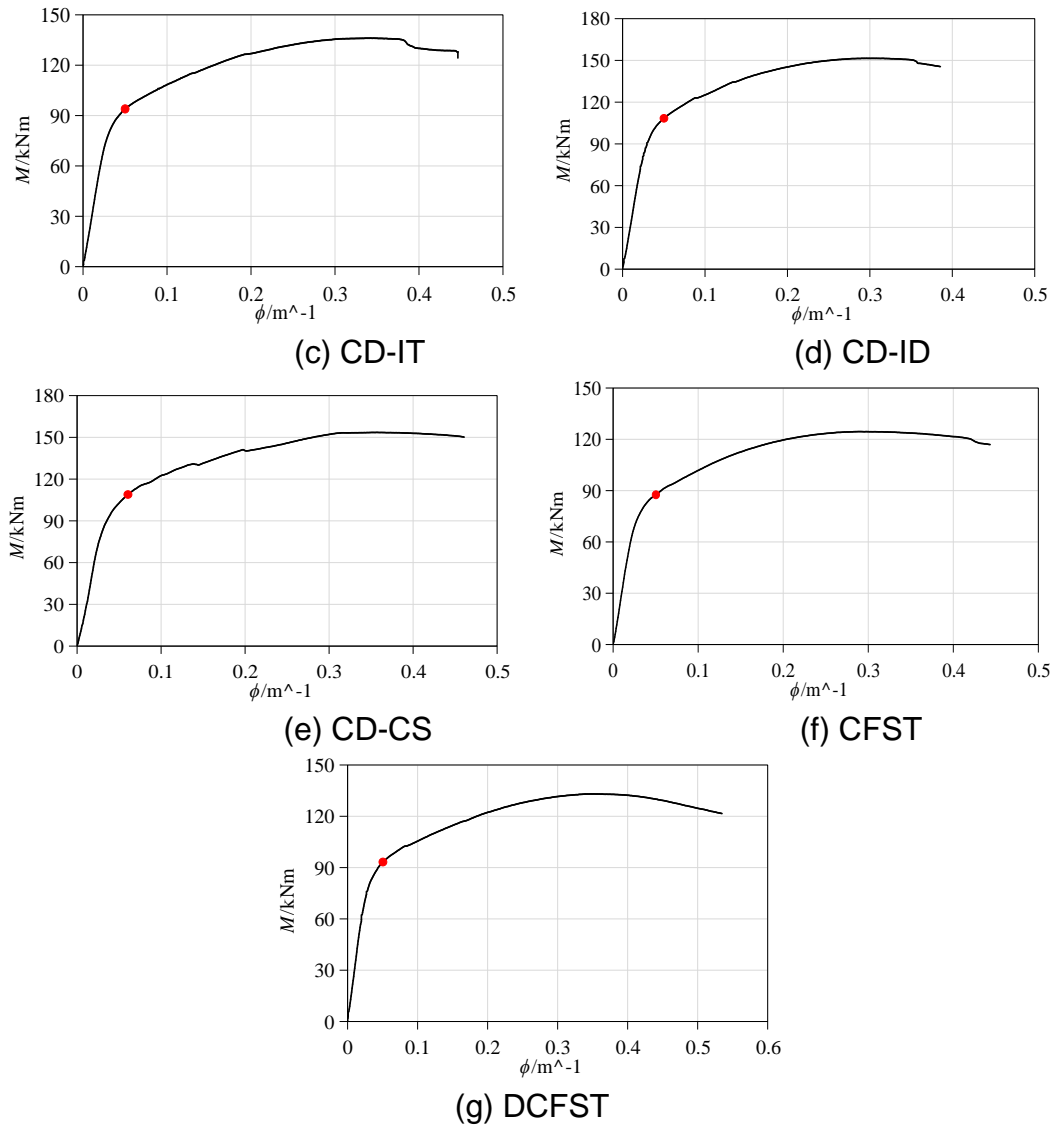
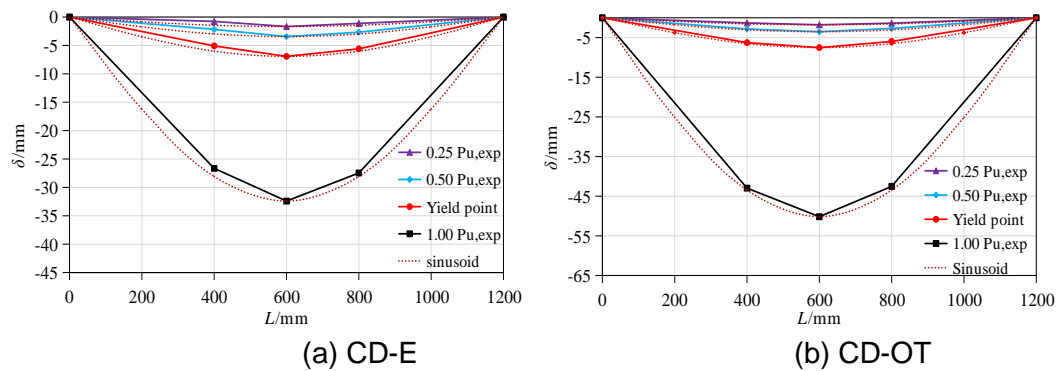


Fig. 6:  $M-\phi$  curves of all tested members.

Figures 7 and 8 present the deflection curves of the test samples with the corresponding sinusoidal half-wave curves. It is seen that the deflection curves of test samples are in good agreement with sinusoidal half-wave curves. Furthermore, the deflection is increased remarkably after the yielding point.



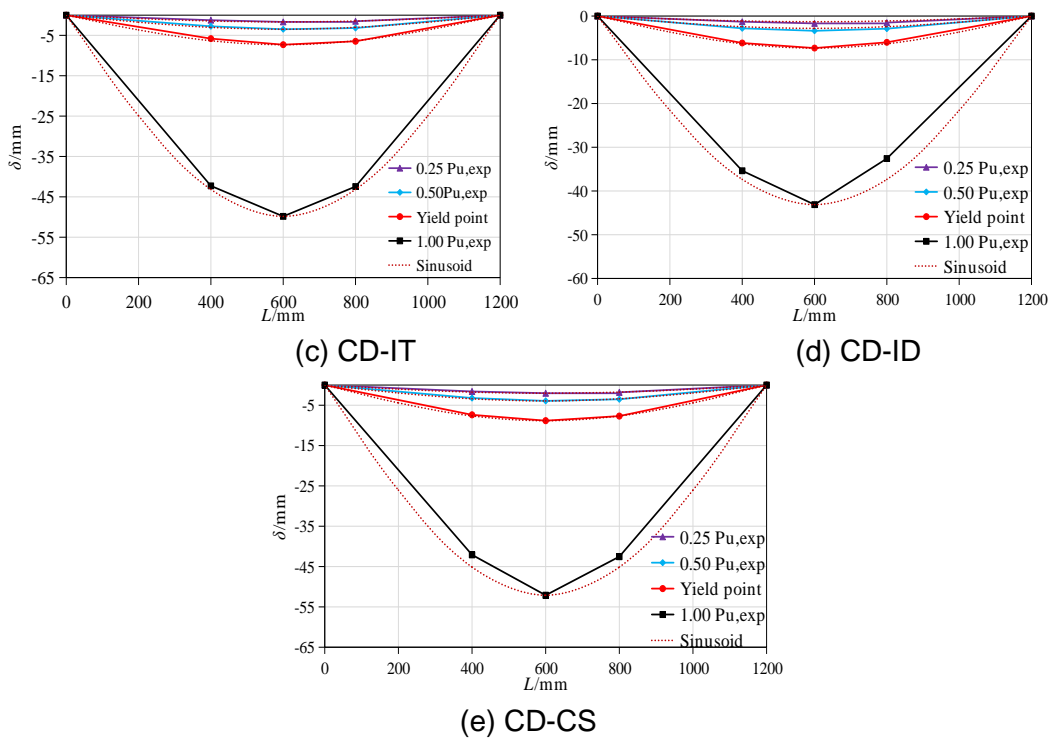


Fig. 7: Deflection curves of CFDST members.

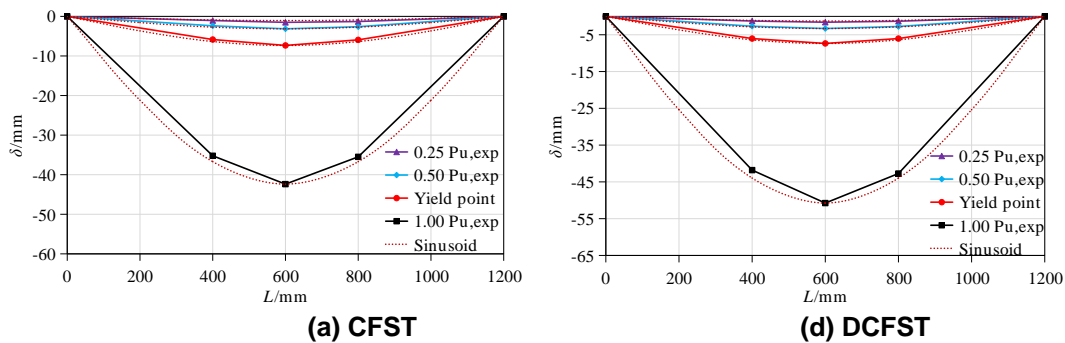


Fig. 8. Deflection curves of CFST and DCFST members.

## CONCLUSIONS

The flexural performance of circular CFDST members has been studied experimentally and reported in this paper. The effects of the thickness of the outer and inner steel tubes, diameter ratio, and the concrete strengths on the flexural performance of CFDST members are studied. The failure of the tested specimens is mainly the buckling of the steel tube at the compression zone. The increase in the steel area improves the flexural capacity of the specimens, however, the influences of the outer tube are much distinguished from other parameters.

## REFERENCES

- [1] Zheng Y.Q, Tao Z., (2019), "Compressive strength and stiffness of concrete-filled double-tube columns", *Thin-Walled Structures*, Vol 134, pp. 174-188.
- [2] Ahmed M, Liang Q.Q, Patel V.I, Handi M.N.S., (2019), "Numerical analysis of axially loaded circular high strength concrete-filled double steel tubular short columns", *Thin-Walled Structures*, Vol. 138, pp. 105-116.
- [3] Ci J.C, Jia H, Chen S.C, Yan W.M, Song T.Y, Kim K.S, (2020), "Performance analysis and bearing capacity calculation on circular concrete-filled double steel tubular stub columns under axial compression", *Structures*, Vol. 25, pp. 554-565.

- 
- [4] Qian J.R, Zhang Y, Ji X.D, Cao W.L., (2011), "Test and analysis of axial compressive behavior of short composite-sectional high strength concrete filled steel tubular columns", *Journal of Building Structures*, Vol. 32, Issue 12, pp 162-9. (in Chinese)
- [5] Ahmed M, Liang Q.Q, Patel V.I, Hadi M.N.S., (2018), "Nonlinear analysis of rectangular concrete-filled double steel tubular short columns incorporating local buckling", *Engineering Structures*, Vol. 175, pp. 13-26.
- [6] Ci J.C, Chen S.C, Jia H, Yan W.M, Song T.Y, Kim K.S., (2020), "Axial compression performance analysis and bearing capacity calculation square concrete-filled double-tube short columns", *Marine Structures*, Vol. 72, pp. 102775.
- [7] Xiong M.X, Xiong D.X, Liew J.R., (2017), "Axial performance of short concrete filled steel tubes with high-and ultra-high-strength materials", *Engineering Structures*, Vol 136, pp. 494-510.
- [8] Ahmed M, Liang Q.Q, Patel V.I, Hadi M.N.S., (2019), "Experimental and numerical studies of square concrete-filled double steel tubular short columns under eccentric loading", *Engineering Structures*, Vol. 197, pp. 109419.
- [9] Ahmed M, Liang Q.Q, Patel V.I, Hadi M.N.S., (2019), "Behavior of eccentrically loaded double circular steel tubular short columns filled with concrete", *Engineering Structures*, Vol. 201, pp. 109790.
- [10] Ahmed M, Liang Q.Q, Patel V.I, Hadi M.N.S., (2020), "Experimental and numerical investigations of eccentrically loaded rectangular concrete-filled double steel tubular columns", *Journal of Constructional Steel Research*, Vol. 167, pp. 105949.
- [11] Pei W.J., (2005), "Research on mechanical performance of multibarrel tube-confined concrete columns", ME Thesis, Chang'an University, Xi'an, China. (in Chinese)
- [12] Qian J.R, Zhang Y, Zhang W.J., (2015), "Eccentric compressive behavior of high strength concrete filled double-tube short columns", *Journal of Tsinghua University*, Vol. 55, issue 1, pp. 1-7.
- [13] Hassanein M.F, Elchalakani M, Patel V.I., (2017), "Overall buckling behaviour of circular concrete-filled dual steel tubular columns with stainless steel external tubes", *Thin-Walled Structures*, Vol. 115, pp. 336-348.
- [14] Ahmed M, Liang Q.Q, Patel V.I, Hadi M.N.S., (2019), "Local-global interaction buckling of square high strength concrete-filled double steel tubular slender beam-columns", *Thin-Walled Structures*, Vol. 143, pp. 106244.
- [15] Ahmed M, Liang Q.Q, Patel V.I, Hadi M.N.S., (2020), "Computational simulation of eccentrically loaded circular thin-walled concrete-filled double steel tubular slender columns", *Engineering Structures*, Vol. 213, pp. 110571.
- [16] GB/T 228.1-2010, (2010), *Metallic materials-Tensile testing-Part 1:Method of test at room temperature*. (in Chinese)
- [17] Feng P, Qiang H.L, Ye L.P., (2017), "Discussion and definition on yield points of materials, members and structures", *Engineering Mechanics*, Vol. 34, issue 3, pp. 36-46.